Preprint Title	Determination of the dielectric constant of non-planar nanostructures and single nanoparticles by Electrostatic Force Microscopy
Authors	Marc Fuhrmann, Anna Musyanovych, Ronald Thoelen and Hildegard Möbius
Publication Date	10 Mai 2022
Article Type	Full Research Paper
ORCID® iDs	Marc Fuhrmann - https://orcid.org/0000-0002-1030-6578; Ronald Thoelen - https://orcid.org/0000-0001-6845-0866; Hildegard Möbius - https://orcid.org/0000-0003-2725-9752

Determination of the dielectric constant of non-planar nanostructures and single nanoparticles by Electrostatic Force Microscopy

Marc Fuhrmann[1], Anna Musyanovych[2], Ronald Thoelen[3,4], Hildegard Moebius*[1]

Address:

[1] Department of Computer Sciences / Micro Systems Technology, University of Applied Sciences Kaiserslautern, Amerikastr. 1, 66482 Zweibrücken, Germany

[2] Chemistry Division, Fraunhofer IMM, Carl-Zeiss-Str. 18-20, 55129 Mainz, Germany

[3] Institute for Materials Research, Hasselt University, Martelarenlaan 42, 3500 Hasselt, Belgium

[4]IMEC vzw, Division IMOMEC, 3590 Diepenbeek, Belgium

Email: Hildegard Möbius – hildegard.moebius@hs-kl.de

* Corresponding author

‡ Equal contributors

Abstract

Electrostatic Force Microscopy has been proven to be a precise and versatile tool to perform quantitative measurements of the dielectric constants of nanoparticles and thin film structures. In this work, an alternative approach based on direct current (DC) linear lift mode is presented. The difference to conventional lift mode measurements is based on the elimination of topographical influences in electrostatic field measurements. Thus, the electrostatic potential penetrating the dielectric material remains constant to accurately predict field changes based solely on the dielectric properties.

1

Measurements of polystyrene (PS), polylactide (PLA) and polymethyl methacrylate (PMMA) nanoparticles show that the presented technique can detect differences in dielectric constants based on material properties.

Keywords

atomic force microscopy; electrostatic force microscopy; polymer nanoparticles; dielectric properties

Introduction

In recent years Electrostatic Force Microscopy (EFM) has attracted more and more attention to determine dielectric constants of thin films [1–3] of interfaces [4,5] nanostructured systems [6] and of nanoparticles [7]. The advantage of using EFM instead of conventional methods such as ellipsometry is the increased lateral spatial resolution, which opens the possibility to map dielectric constants in the nanometer range. Nevertheless, it is limited to very smooth surfaces as the surface induces topographic crosstalks falsifying the obtained dielectric constants [8]. The EFM (phase or frequency) signal often resembles the topography as reported in various publications [1,6,9]. This effect is also observed in Magnetic Force Microscopy (MFM) [10,11]. In both methods, EFM and MFM, the cause for the topographic crosstalk is the same namely capacitive coupling effects between tip and substrate due to the mode of operation, the so-called lift mode. EFM and MFM measurements are based on scanning a surface with a tip oscillating with a frequency near to its resonance frequency in a two-pass technique [12]. In a first scan, the tapping mode, the tip touches the surface in its lowest point thus the topography of the sample becomes visible. In a second scan, EFM and MFM measurements usually are performed in the

lift mode in a certain distance from the surface, the so-called lift height, following the topography profile from the first scan. Thus, short-range forces are no longer relevant and the long-range forces such as magnetic and electrostatic forces can be determined. Common to all methods is the fact that tip and substrate form a capacitor. Thus, changes in distance between substrate and tip due to non-planar structures lead to a decrease in the electrostatic force when the distance increases and an increase in the electrostatic force when the distance decreases, resulting in a significant contribution of topography to the EFM or MFM signal. For MFM measurements various methods to reduce capacitive coupling contributions are discussed e.g., reducing the tip size or including a dielectric layer between the substrate and the nanostructure to be investigated or changing the tip magnetization [13–15]. In order to investigate the magnetism of nanoparticles, it was shown that while embedding the nanoparticles, the crosstalk due to capacitive coupling dissapears[16]. In earlier work [17], an algorithm was developed to correct MFM lift mode data based on a correlation of the AFM signal and the MFM signal. A similar method was developed by van der Hofstadt for lift mode electrostatic force microscopy of non-planar samples [8]. Their algorithm subtracts the contributions of topographic crosstalk from EFM signals. This method was successfully applied to locally determine the dielectric constant of silicon dioxide pillars as well as of single bacterial cells [8]. Many groups determined the dielectric constant of thin films by EFM [1,5,18]. Gomila et al extracted the topographic crosstalk by subtracting the signal beside the thin film from the signal above the thin film, thus determining the so-called intrinsic capacitance [3]. Gramse et al reported the topographic crosstalk for planar structures. In EFM exist three possibilities to determine the dielectric constant, the use of the DC-signal and the use of two possible alternating current (AC) signals, the $\Delta\Phi$ (ω) phase signal and the $\Delta\Phi$ (2ω) phase signal. In all methods the force is proportional to the first derivative of the capacitance which is related to the dielectric

constant. All methods have their advantages and disadvantages. Gramse et al further reported the advantage of using the DC signal because of no need for additional electronics. The use of the AC signals has the advantage to be independent of the contact potential difference between tip and sample. Common to all three methods is the topographic crosstalk initiated by the mode of operation, namely the lift mode.

One possibility to avoid topographic crosstalk is the use of the linear mode instead of the lift mode. In this paper we compare linear and lift mode measurements in EFM theoretically as well as in experiments on various structures. EFM phase signals of dielectric layers with trench-structures reveal that lift mode measurements reduce the sensitivity to measure the dielectric constant significantly, whereas linear mode measurements allow the determination of the dielectric constant of the layer. In principle, the determination of the dielectric constant of nanoparticles is not possible in lift mode measurements, because the change in distance between tip and substrate changes the effective area of the capacitor as proven in [15], so that the contribution of the nanoparticle to the dielectric contrast becomes too small to be detected. In this paper we determined the dielectric constant of polystyrene (PS), polylactide (PLA) and polymethyl methacrylate (PMMA) nanoparticles with linear mode measurements. It is shown that the contrast in linear mode is independent of the tip form and tip size. In general, it is experimentally proven that the topographic crosstalk often seen in EFM measurements on non-planar nanoscale structures can be avoided by using the linear mode instead of the lift mode, thus allowing the determination of the dielectric constant of nanoscale structures.

Results and Discussion

EFM includes different methods to determine the electrical properties such as the dielectric constant via electrical excitation of the tip by DC or AC voltage. For both the DC or AC voltage, the force acting on the tip is proportional to the first derivative of the capacitance between tip and sample. Accordingly, all methods are sensitive to changes in capacitance due to changes of the dielectric constant. As mentioned above EFM measurements can be performed in two modes: the so-called lift mode following the topography of the first topographic scan in a defined distance as a second scan trace and the so-called linear mode with a fixed distance between tip and substrate. In this paper we focus on theory and measurements using DC voltage, but the comparison of lift and linear modes is valid for AC signals as well and can be easily transferred to these methods.

Dielectric contrast of non-planar surface structures in lift- and linear mode measurements

Non-planar dielectric surface structures contribute to the EFM-phase signal in lift mode measurements twice: a first contribution is induced by a change of the volume fraction of the dielectric material in the tip-sample capacitor forming a dielectric contrast. A second contribution derives from the distance change between tip and substrate following the topography of the sample, as indicated in Figure 1. This leads to an additional force on the tip as well as to a change of the effective area A_{eff} of the tip-sample capacitor. Increasing the distance between tip and substrate leads to a positive phase shift, whereas decreasing the distance leads to a negative phase shift [19]. Additionally, A_{eff} has to be adapted as a function of the distance between tip and substrate as described in [19].

Increasing the distance between tip and substrate increases A_{eff} as reported in [14,19]. Both contributions are taken into account in equation (1) in Table 1 which gives the phase signal as a function of the topographic parameter and the dielectric constant. In this paper we use a parabolic tip model as described in our previous works in order to calculate A_{eff} [17,19]. Measurements in lift mode always include contributions from the topography reducing the sensitivity to determine the dielectric contrast. The influence of the topography decreases for films with non-planar nanostructures with heights small compared to the total thickness of the dielectric layer as shown in Figure 1 and discussed in [15]. Figure 1 depicts the dependence of the phase signal for a nanostructure with 50 nm height as a function of the thickness of the dielectric layer beneath the nanostructure. A layer thickness of 300 nm can reduce topographic crosstalk in lift mode measurements by a factor of ten.
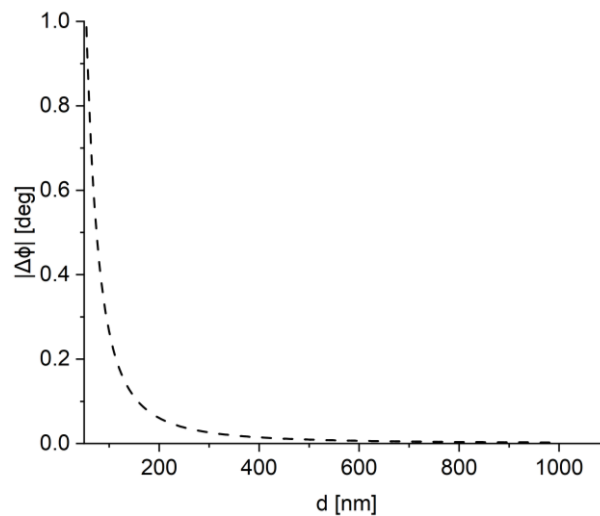
Figure 1: Absolute value of phase shift as a function of dielectric layer thickness

In contrast to the lift mode, linear mode measurements keep the distance between tip and substrate constant during the measurement, removing the influence of the topography on the phase signal. Therefore, the phase shift resulting from the electrostatic coupling between tip and substrate is only dependent on the amount of

dielectric material within the capacitor. Thus, in linear mode measurement the only contrast is a dielectric contrast, whereas in lift mode measurements the contrast has two overlapping contributions, from topography and from the dielectric material, in the capacitor reducing the sensitivity for the determination of the dielectric constant. Table 1 shows the differences in the measurement methods and how they affect the calculations.

Table 1: Comparison of lift mode and linear mode for non-planar dielectric (nano)-structures and the corresponding equations for the phase shift.

	Lift Mode	Linear Mode
Scheme		

Equation

Lift Mode:
$$\Delta\phi = -\frac{Q}{k}\epsilon_0(V_{tot})^2\left(\frac{A_{eff}}{\left(z+\frac{d+t_{topo}}{\epsilon_l}\right)^3} - \frac{A_{eff}}{\left(z+\frac{d}{\epsilon_l}\right)^3}\right) \quad (1)$$

Linear Mode:
$$\Delta\phi = -\frac{Q}{k}\epsilon_0(V_{tot})^2\left(\frac{A_{eff}}{\left((z-t_{topo})+\frac{d+t_{topo}}{\epsilon_l}\right)^3} - \frac{A_{eff}}{\left(z+\frac{d}{\epsilon_l}\right)^3}\right) \quad (2)$$

$$A_{eff} = \pi r_{eff}^2 \text{ with } r_{eff} = \sqrt{\left(\sqrt[3]{\frac{z_1^3}{p}}\right)r_{tip}} \quad (3)$$

$$z_1(x,y) = z + d + t_{topo}(x,y) \quad (4) \qquad\qquad z_1(x,y) = z + d \to const \quad (5)$$

Legend

|					
Q	cantilever quality factor	V_{tot}	$V_{CPD} + V_{Tip}$	$t_{topo}(x,y)$	topography parameter
k	spring constant	A_{eff}	effective area of the capacitor	$t_{topo} = 0$	baseline of the topography
ϵ_0	vacuum dielectric	d	dielectric layer thickness	p	percentage factor
ϵ_l	dieletric layer constant	z	lift height	r_{tip}	tip radius

Measurements of thin film structures of 60 nm spin coated ARP-5910 positive-photoresist demonstrate the difference of lift mode and linear mode measurements on non-planar nanostructures. All measurements are performed with a lift height of 20 nm to avoid distortions of short-range forces while still being close enough to detect phase shifts due to material changes.

Table 2 compares lift mode and linear mode measurements of a trench structure with a width of 1.2 µm. In lift mode measurements (Table 2 left) we observe a negative phase signal. According to equation 1 this phase signal consists of a negative contribution due to the decreasing distance between the tip and substrate and a positive contribution due to less dielectric material in the tip-substrate capacitor while measuring above the trench. Considering a trench, the tip is getting closer to its counter plate and, therefore, has a stronger attraction towards the substrate and a respective negative phase. This negative phase signal overlaps the positive phase signal based on the dielectric contrast lowering the resolution.

Instead, in linear mode, only the dielectric contrast contributes to the phase signal (Table 2 right). Due to less dielectric material in the capacitor the phase signal is positive and larger than the phase signal in lift mode measurements as there is no contravise contribution of the topography. Fitting the measured cross-section in the linear mode by using equation 2. In Table 1 we obtained a dielectric constant in the range 2.9 – 3.1 for the ARP-5910 resist. This is in accordance with the original value provided by Allresist GmbH.

Table 2: Comparison of lift mode (left) and linear mode (right) phase shift data for non-planar dielectric (nano)-structures

Lift Mode	Linear Mode
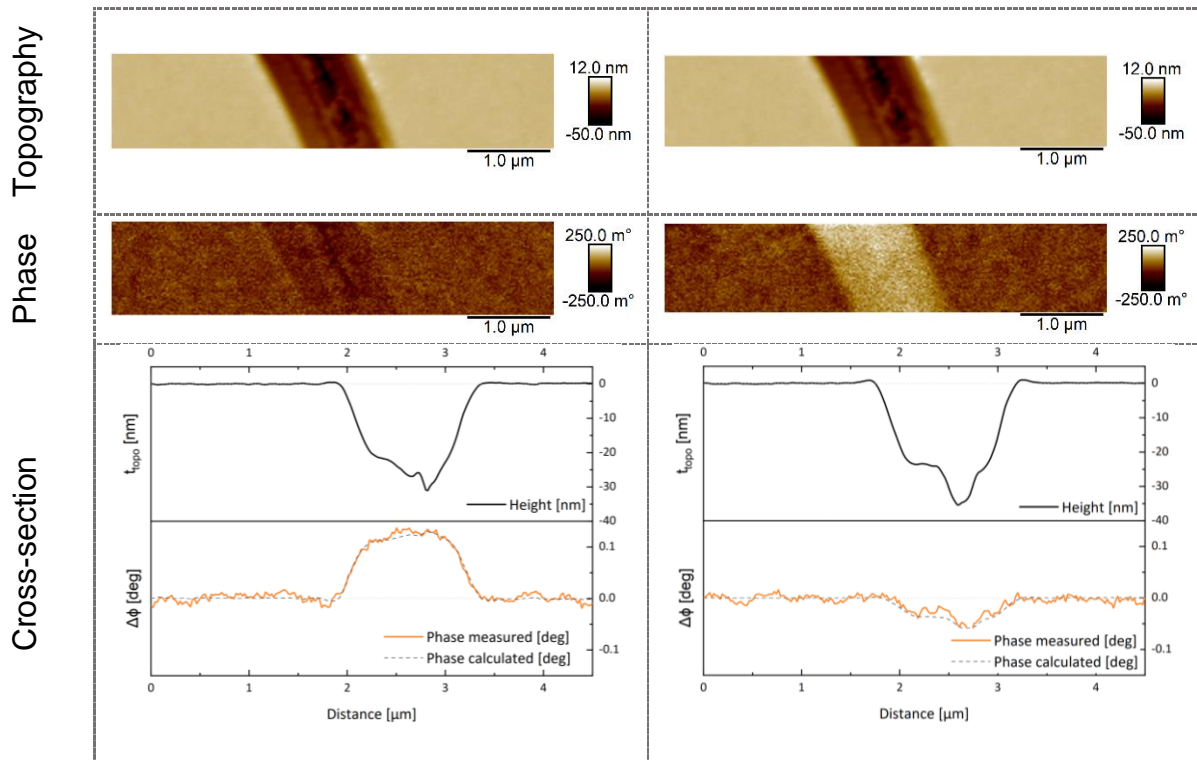
These measurements demonstrate the advantage of using the linear mode to determine dielectric properties of non-planar nanostructures.

Dielectric contrast of single nanoparticles in lift- and linear mode measurements

As described above, in lift mode the distance between tip and sample is kept constant during the measurement following the topography of the sample. Thus, nanoparticles on the surface of the substrate lead to an increasing distance between tip and substrate, resulting in a positive phase shift calculated by equation 6 (Table 3), which induces a topographic contrast in the EFM signal. Note that the sign of the phase shift is always relative to the starting height z of the second trace. Investigations on the influence of the dielectric constant on the topographic crosstalk showed that the dielectric constant of the nanoparticle has no significant influence on the topographic crosstalk [19]. The reason for this is the fact that with increasing particle diameter the effective area of the tip-substrate capacitor increases as well due to the increasing

distance between tip and substrate. Thus, the volume fraction of the nanoparticle in the capacitor stays constant and small compared to the volume of the total capacitor. This effect hinders in principle the determination of the dielectric constant of nanoparticles in lift mode measurements. Applying an additional external voltage leads to an increase of the phase signal resulting in an upward opened parabola (Table 4) initiated by the topographic contrast. The contact potential voltage V$_{CPD}$ is given by the vertex of the parabola.

Considering the electrostatic forces for single nanoparticles measured in linear mode, the signal is only due to the contribution of the dielectric constant of the nanoparticle in the tip-sample capacitor, equation 7 in Table 3: In this case the dielectric contrast of the nanoparticle leads to a negative phase shift. Therefore, linear mode measurements enable the determination of the dielectric constant of single nanoparticles based on these capacitive effects mentioned above.

Table 3: Comparison of Lift mode and linear mode for a single polymer nanoparticle and corresponding equations for the phase shift.

	Lift Mode	Linear Mode
Scheme		
Equation	$\Delta\phi = -\dfrac{Q}{k}\epsilon_0(V_{tot})^2\left(\dfrac{A_{eff}}{\left(z+\frac{d}{\varepsilon_p}\right)^3} - \dfrac{A_{eff}}{(z)^3}\right)$ (6)	$\Delta\phi = -\dfrac{Q}{k}\varepsilon_0(V_{tot})^2\left(\dfrac{A_{exp}}{\left(z+\frac{d}{\varepsilon_p}\right)^3} - \dfrac{A_{exp}}{(z+d)^3}\right)$ (7)
	$A_{eff} = \pi r_{eff}^2$ with $r_{eff} = \sqrt{\left(\sqrt[3]{\frac{z_1^3}{p}}\right)r_{tip}}$ (3)	$A_{exp} = \pi r_{exp}^2$ (9)

	$z_1(x,y) = z + d$ (4)			$z_1(x,y) = z + d \rightarrow const$ (5)	
Legend	**Q** cantilever quality factor	**V_tot** $V_{CPD} + V_{Tip}$	**A_exp** experimental half-width area of particle		
	k spring constant	**A_eff** effective area of the capacitor	**r_eff** experimental half-width radius of particle		
	ε_0 vacuum dielectric	**d** particle diameter	**p** percentage factor		
	ε_p dielectric constant of particle	**z** lift height	**r_tip** tip radius		

In linear mode measurements tip form and size are less important than in the lift mode as the distance between tip and substrate stays constant. Therefore, A_{eff} is a constant pre-factor in equation 7. A_{eff} can be calculated by the parabolic tip model in equation 3 used for the calculation of the phase signal in the lift mode. But this equation requires knowledge of the exact value of the tip radius. In order to determine A_{eff} without knowing the exact value of the tip radius the following method of analysis can also be used. Tip size and form are taken into account by using the half-width of the measured topographic cross-section of the nanoparticles. The half-width includes the convolution of the tip and the nanoparticle. This method allows to gain r_{eff} without knowing the actual tip form and radius. The values obtained are in accordance with the parabolic tip model. According to Markiewiecz, assuming spherical geometries for tip and sample, the half-width w_h can be calculated as [20]:

$$w_h{}^2 = r_{tip}4d \tag{11}$$

with

r_{tip}: radius of the tip

d: measured height (= diameter of the nanoparticle)

$$w_h = 2r_{eff} \qquad\qquad\qquad\qquad\qquad (12)$$

r_{eff}: measured half-width of the nanoparticle

In order to demonstrate the independence of this method from tip size and form and from particle size and material we compared three particle groups (PS, PMMA and PLA) with different particle diameter in the range from 80 nm to 200 nm measured with three different tips (Table 3). Figure 2 shows the measured half-width of the nanoparticles as a function of the diameter of the nanoparticle. The calculated line is based on the Markiewiecz formula (equation 11), and the tip radius was determined by SEM. All measurements were within a 10% tolerance band within the Markiewiecz calculation.
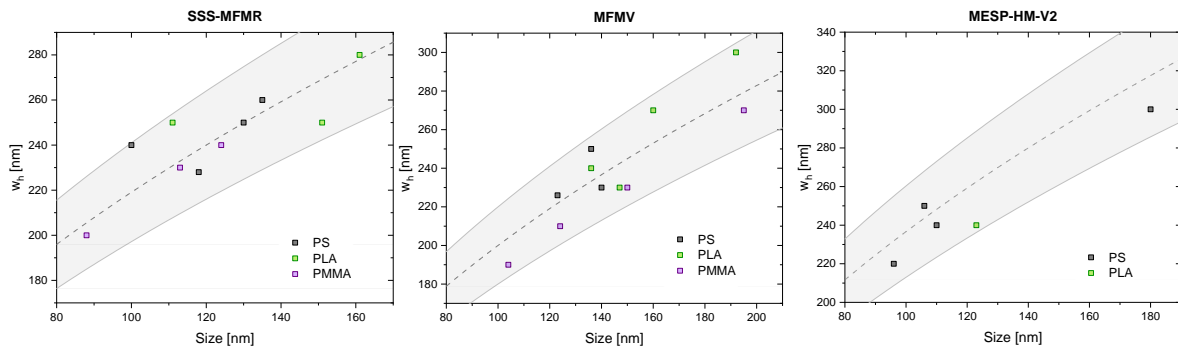

Figure 2: Half-width of PS, PLA and PMMA particles with different tips (Radius: SSS-MFMR – 15 nm; MFMV – 40 nm; MESP-HM-V2 – 80 nm)

Table 4 compares lift and linear mode measurements for PS particles.

While the phase signal clearly shows the influence of capacitive coupling due to distance changes, linear mode measurements proof that measuring nanoparticles at a

lift height of 20 nm above the sample only show a small negative phase shift for V = 0 based on the dielectric contrast. In order to enhance the dielectric contrast, an electrostatic field is applied between tip and substrate in the range of -2V and +2V. As this dielectric contrast is directly proportional to the voltage between tip and substrate, an additional external voltage leads to an increase of the phase signal resulting in a downwards opened parabola as shown in Table 4.

Table 4: Comparison of Lift-Mode and Linear-Mode phase shift data for a single polymer nanoparticle

Voltage Profile
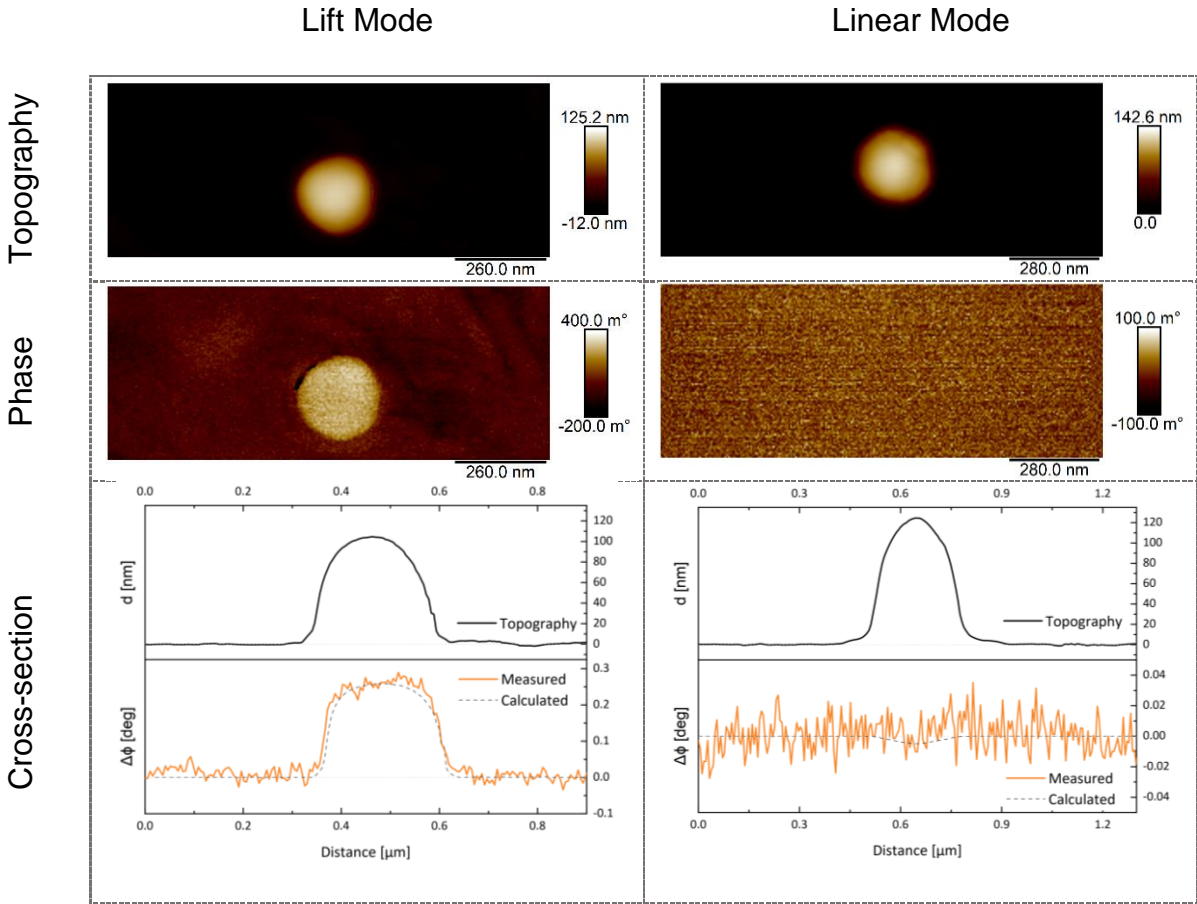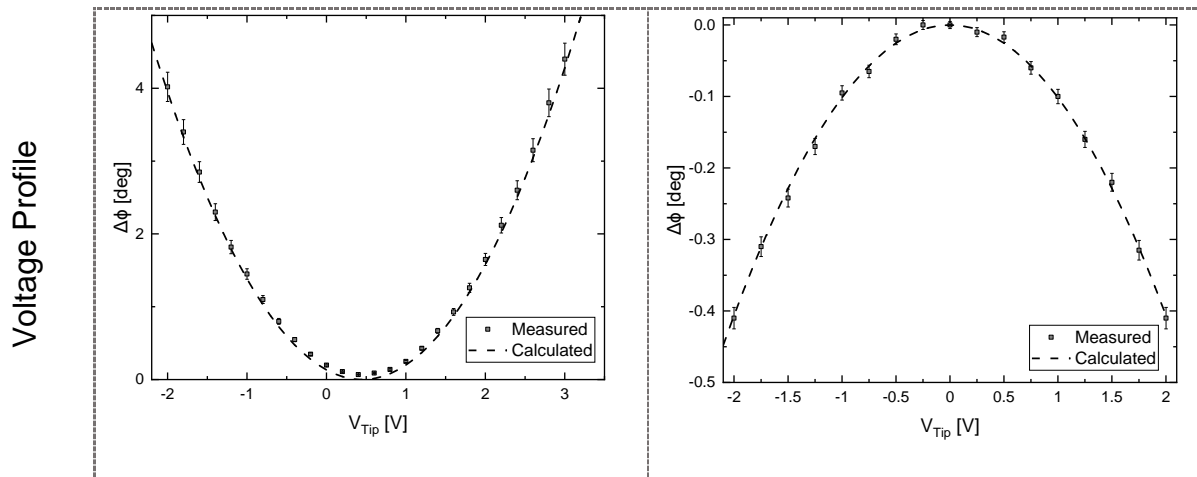
Determination of dielectric constant based on linear mode measurements

Analysis of the parabola in Table 4 measured in linear mode now allows to determine the dielectric constant of single nanoparticles. In this paper we investigated different polymer nanoparticles made of PS, PMMA or PLA with a size in the range of 80 nm – 200 nm investigated with three different tips (Table 5). The dielectric constant is the only fit parameter in equation 7, V_{CPD} is determined by the vertex of the parabola, the diameter of the particle by the topographic height and A_{eff} determined by the half-width of the topographic cross-section, r_{eff}. Figure 3 summarizes the results of these measurements:
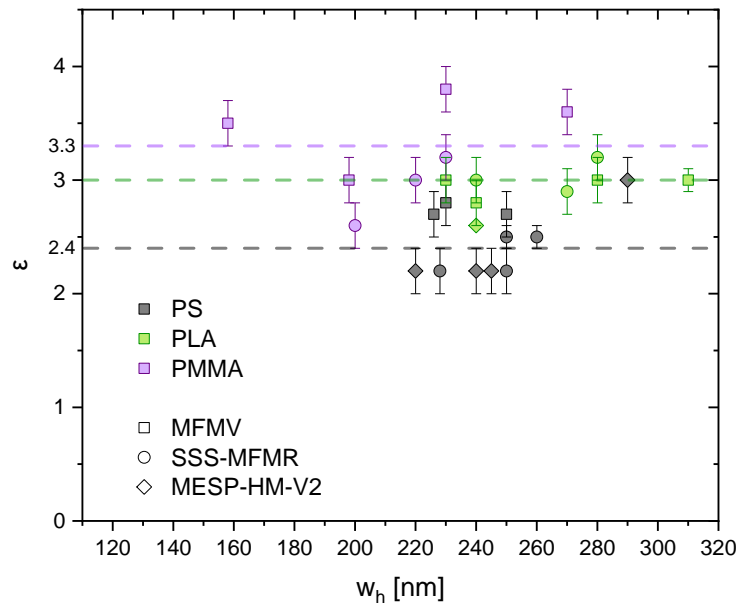
Figure 3: Evaluation of the dielectric constant of nanoparticles of different material and size and of different measuring tips based on voltage profile measurements.

The average values of the three materials investigated are $\varepsilon = 2.4 \pm 0.19$ for polystyrene, $\varepsilon = 3 \pm 0.24$ for polylactide and $\varepsilon = 3.3 \pm 0.26$ for polymethyl methacrylate. These values are in accordance with the literature [21] and [22].

Conclusion

In summary we could demonstrate the influence of topographic crosstalk on lift mode EFM measurements of thin films with non-planar nanostructures. The topographic crosstalk vanishes with increasing dielectric layer thickness between nanostructure and substrate. Topographic contrast can completely be avoided by using the linear mode instead of lift mode for the determination of dielectric properties. It was shown that the dielectric constant of nanoparticles cannot be determined in lift mode

measurements, since the change in distance between the tip and substrate has so much greater effect on the signal that the dielectric contrast cannot be measured. Linear mode measurements allow the determination of the dielectric constant of nanoparticles independent of tip form and size. To enhance the contrast, it is necessary to apply a voltage between tip and substrate.

Experimental

Polystyrene (PS), polymethyl methacrylate (PMMA) and polylactide (PLA) particles in a size-range of 80 nm – 200 nm were studied in regard to the dielectric constant. PS and PMMA nanoparticles were synthesized by miniemulsion polymerization with the non-ionic surfactant Lutensol AT50 to ensure a lower zeta potential [23]. Briefly, 3 g of styrene or methyl methacrylate, 125 mg of hexadecane and 60 mg of the initiator 2,20-azobis(2-methylbutyronitrile) (V59) were mixed together and added to 24 g of water containing 200 mg of non-ionic surfactant Lutensol AT50, which is a poly(ethylene oxide)-hexadecylether with an EO block length of 50 units (BASF). After stirring 1 h for pre-emulsification at 900 rpm, the miniemulsion was prepared by ultrasonicating the mixture for 120 s at 90% amplitude (Branson sonifier W450 Digital, ½". tip) in ice bath to prevent the polymerization. The polymerization was carried out at 72 °C over night under stirring at 400 rpm.

PLA nanoparticles were prepared by combination of miniemulsion and solvent evaporation methods. Briefly, 0.3 g of PLA were dissolved in 10 g of chloroform and added to 24 g of water containing 72 mg of sodium dodecyl sulfate. After stirring 1 h for pre-emulsification at 900 rpm, the miniemulsion was prepared by ultrasonicating the mixture for 180 s at 70% amplitude in a pulse regime (30 s sonication, 10 s pause) using 1/4" tip. The obtained miniemulsion was transferred to the 50 ml round bottom

reaction flask and left overnight at 40 °C for complete evaporation of chloroform. The obtained nanoparticles were purified by centrifugation to remove the excess of surfactant and characterized in terms of particles size and zeta potential. Zeta potentials were -1 mV, - 8 mV and -49 mV for PS, PMMA and PLA nanoparticles, respectively. The nanoparticle dispersions were diluted with highly purified water (1 µl dispersion with 10 ml water) to avoid aggregation and then dropped 30 µl on a freshly cleaved siegert wafer for drying. Morphological verification of the nanoparticles with regards to sphericity and deformation were performed by TEM and AFM measurements.

All dielectric constant measurements were performed on a Dimension Icon AFM with tips of different radii. The radii ranged from 15 nm up to 80 nm with quadrilateral pyramidic shape, which were validated by scanning electroscope microscopy measurements. Measurements to determine dielectric properties were performed in EFM mode with a scan rate of 1 Hz. Imaging resolution was set to 512 samples per line. The two-pass scan collects topography information using tapping mode and electrostatic information in linear mode with a lift height of 20 nm above the particle. For calculation and illustation purposes, topography data was extracted as X,Z-data and evaluated by using the data analysis program OriginPro. As described above, linear mode eliminates topographic crosstalk caused by capacitive coupling and allows an estimation of the dielectric constant. In this mode, the tip scans the surface in two steps. In a first trace the surface profile of a scan line is rastered by tapping mode. In standard lift mode, this profile is used for the second trace to maintain a constant distance between the tip and the surface. The linear mode used for the determination of the dielectric properties, on the other hand, ignores the topography information. Only a fixed distance is set, which is independent of the topography. It is therefore always important to know the sample exactly in order to avoid tip crashes and the resulting

destruction of structures and measuring tips. To verify the acquired data, KPFM measurements were performed to match the V_{CPD} values resulting from the linear mode measurements with those of the conventional KPFM measurements.

Considering various tip radii, it is important to include the convolution error in the calculations. Spring constant k of each tip type as well as its quality factor must be matched for each individual measurement due to the determining pre-factor when calculating then phase shift. The quality factor is determined during the Cantilever Tune setup based on the characteristics of the resonance frequency. These essential parameters for the calculation of the phase shift are summarized in Table 5.

Table 5: Parameters of commercial tips used for measurements: tip radius r, resonance frequency f_r, spring constant k and quality factor Q

Probe	Company	r/nm	f_r/kHz	k/Nm^{-1}	Q-factor
SSS-MFMR	Nanosensors	15	75	2,8	190-220
MFMV	Bruker AFM Probes	40	75	2,8	240 - 260
MESP-HM-V2	Bruker AFM Probes	80	75	3	240 - 260

Acknowledgements

Funding

References

1. Gramse, G.; Casuso, I.; Toset, J.; Fumagalli, L.; Gomila, G. Quantitative Dielectric Constant Measurement of Thin Films by DC Electrostatic Force. *Nanotechnology* **2009**, *20*, 395702, doi:10.1088/0957-4484/20/39/395702.

2. Sadewasser, S.; Barth, C. Electrostatic Force Microscopy And Kelvin Probe Force Microscopy. *Characterization of Materials* **2012**, 1–12, doi:10.1002/0471266965.COM152.

3. Gomila, G.; Toset, J.; Fumagalli, L. Nanoscale Capacitance Microscopy of Thin Dielectric Films. *Journal of Applied Physics* **2008**, *104*, 024315, doi:10.1063/1.2957069.

4. Labardi, M.; Bertolla, A.; Sollogoub, C.; Casalini, R.; Capaccioli, S.; Capaccioli, S.; Capaccioli, S. Lateral Resolution of Electrostatic Force Microscopy for Mapping of Dielectric Interfaces in Ambient Conditions. *Nanotechnology* **2020**, *31*, doi:10.1088/1361-6528/AB8EDE.

5. Peng, S.; Zeng, Q.; Yang, X.; Hu, J.; Qiu, X.; He, J. Local Dielectric Property Detection of the Interface between Nanoparticle and Polymer in Nanocomposite Dielectrics. *Scientific Reports* **2016**, *6*, doi:10.1038/srep38978.

6. Valeriano, W.W.; Andrade, R.R.; Vasco, J.P.; Malachias, A.; Neves, B.R.A.; Guimaräes, P.S.S.; Rodrigues, W.N. Mapping the Local Dielectric Constant of a

Biological Nanostructured System. *Beilstein journal of nanotechnology* **2021**, *12*, 139–150, doi:10.3762/BJNANO.12.11.

7. Gomila, G.; Esteban-Ferrer, D.; Fumagalli, L. Quantification of the Dielectric Constant of Single Non-Spherical Nanoparticles from Polarization Forces: Eccentricity Effects. *Nanotechnology* **2013**, *24*, doi:10.1088/0957-4484/24/50/505713.

8. van der Hofstadt, M.; Fabregas, R.; Biagi, M.C.; Fumagalli, L.; Gomila, G. Nanoscale Dielectric Microscopy of Non-Planar Samples by Lift-Mode Electrostatic Force Microscopy. *Nanotechnology* **2016**, *27*, doi:10.1088/0957-4484/27/40/405706.

9. Tevaarwerk, E.; Keppel, D.G.; Rugheimer, P.; Lagally, M.G.; Eriksson, M.A. Quantitative Analysis of Electric Force Microscopy: The Role of Sample Geometry. *Review of Scientific Instruments* **2005**, *76*, doi:10.1063/1.1898183.

10. Schwarz, A.; Wiesendanger, R. Magnetic Sensitive Force Microscopy. *Nano Today* **2008**, *3*, 28–39, doi:10.1016/S1748-0132(08)70013-6.

11. Jaafar, M.; Asenjo, A. Unraveling Dissipation-Related Features in Magnetic Imaging by Bimodal Magnetic Force Microscopy. *Applied Sciences 2021, Vol. 11, Page 10507* **2021**, *11*, 10507, doi:10.3390/APP112210507.

12. Vokoun, D.; Samal, S.; Stachiv, I. Magnetic Force Microscopy in Physics and Biomedical Applications. *Magnetochemistry* **2022**, *8*, 42, doi:10.3390/MAGNETOCHEMISTRY8040042.

13. Angeloni, L.; Passeri, D.; Reggente, M.; Mantovani, D.; Rossi, M. Removal of Electrostatic Artifacts in Magnetic Force Microscopy by Controlled Magnetization of the Tip: Application to Superparamagnetic Nanoparticles. *Scientific Reports* **2016**, *6*, 26293, doi:10.1038/srep26293.

14. Krivcov, A.; Junkers, T.; Möbius, H. Understanding Electrostatic and Magnetic Forces in Magnetic Force Microscopy: Towards Single Superparamagnetic

Nanoparticle Resolution. *Journal of Physics Communications* **2018**, *2*, 075019, doi:10.1088/2399-6528/aad3a4.

15. Krivcov, A.; Ehrler, J.; Fuhrmann, M.; Junkers, T.; Möbius, H. Influence of Dielectric Layer Thickness and Roughness on Topographic Effects in Magnetic Force Microscopy. *Beilstein Journal of Nanotechnology* **2019**, *10*, 1056–1064, doi:10.3762/bjnano.10.106.

16. Krivcov, A.; Schneider, J.; Junkers, T.; Möbius, H. Magnetic Force Microscopy of in a Polymer Matrix Embedded Single Magnetic Nanoparticles. *physica status solidi (a)* **2019**, *216*, 1800753, doi:10.1002/pssa.201800753.

17. Fuhrmann, M.; Musyanovych, A.; Thoelen, R.; von Bomhard, S.; Möbius, H. Magnetic Imaging of Encapsulated Superparamagnetic Nanoparticles by Data Fusion of Magnetic Force Microscopy and Atomic Force Microscopy Signals for Correction of Topographic Crosstalk. *Nanomaterials 2020, Vol. 10, Page 2486* **2020**, *10*, 2486, doi:10.3390/NANO10122486.

18. Arinero, R.; Riedel, C.; Schwartz, G.A.; Lévêque, G.; Alegría, A.; Tordjeman, P.; Israeloff, N.E.; Ramonda, M.; Colmenero, J. *Measuring Dielectric Properties at the Nanoscale Using Electrostatic Force Microscopy*; 2009.

19. Fuhrmann, M.; Krivcov, A.; Musyanovych, A.; Thoelen, R.; Möbius, H. The Role of Nanoparticles on Topographic Cross-Talk in Electric Force Microscopy and Magnetic Force Microscopy. *physica status solidi (a)* **2020**, *217*, 1900828, doi:10.1002/pssa.201900828.

20. Markiewicz, P.; Goh, M.C. Simulation of Atomic Force Microscope Tip–Sample/Sample–Tip Reconstruction. *Journal of Vacuum Science & Technology B: Microelectronics and Nanometer Structures Processing, Measurement, and Phenomena* **1998**, *13*, 1115, doi:10.1116/1.587913.

21. Kumar, B.; Kaushik, B.K.; Negi, Y.S. Perspectives and Challenges for Organic Thin Film Transistors: Materials, Devices, Processes and Applications. *Journal of Materials Science: Materials in Electronics* **2014**, *25*, 1–30, doi:10.1007/S10854-013-1550-2/FIGURES/28.

22. Huber, E.; Mirzaee, M.; Bjorgaard, J.; Hoyack, M.; Noghanian, S.; Chang, I. Dielectric Property Measurement of PLA. *IEEE International Conference on Electro Information Technology* **2016**, *2016-August*, 788–792, doi:10.1109/EIT.2016.7535340.

23. Musyanovych, A.; Dausend, J.; Dass, M.; Walther, P.; Mailänder, V.; Landfester, K. Criteria Impacting the Cellular Uptake of Nanoparticles: A Study Emphasizing Polymer Type and Surfactant Effects. *Acta Biomaterialia* **2011**, *7*, 4160–4168, doi:10.1016/J.ACTBIO.2011.07.033.